



Thermal transport in H-terminated ultrathin [110] Si nanowires: a first principles study

Konstanze R. Hahn¹ , Claudio Melis^{1,a} , Fabio Bernardini¹ , Lorenzo Paulatto² , Luciano Colombo¹

¹ Department of Physics, University of Cagliari, Cittadella Universitaria, 09042 Monserrato, CA, Italy

² CNRS, Institut de Minéralogie, de Physiques des Matériaux et de Cosmochimie, IMPMC, Sorbonne Université, UMR 7590, 4 Place Jussieu, 75252 Paris Cedex 05, France

Received: 26 April 2023 / Accepted: 2 November 2023

© The Author(s) 2023

Abstract Phonon properties of ultrathin Si nanowires in [110] direction have been calculated by density functional perturbation theory. Several samples with varying diameters ranging from 0.38 to 1.5 nm have been investigated. It is found that the frequencies of optical phonons at the zone center increase with decrease in size of the nanowire, giving rise to avoided-crossing with longitudinal acoustic phonons. This feature determines a corresponding increase in the scattering rates and flattening of the longitudinal acoustic mode. More specifically, a remarkable change in scattering rates is shown for decreasing diameter. Results of the thermal conductivity are much lower with respect to bulk Si and are found between 40 and 119 Wm⁻¹ K⁻¹, also providing evidence of increasing thermal conductivity with increase in diameter. This effect is attributed to several changes in the phonon dispersions. Finally, it is shown that approximating the boundary scattering of phonons by Casimir scattering leads to a severe underestimation of the thermal conductivity in these systems.

1 Introduction

Silicon nanowires have been extensively investigated [1–3] since they represent an excellent test bed to study the fundamental physics of low-dimensional systems where confinement plays a major role. In addition, their physical properties make them promising candidates for numerous next-generation technologies [4, 5]. In this perspective, their thermal transport properties represent a key issue for many applications [6]. For instance, reducing the dimensions to the nanoscale can lower the thermal conductivity and increase the thermoelectric efficiency. Control of thermal transport is of great importance as well in photovoltaic and microelectronic devices [7–9] where, on the contrary, a high thermal conductivity is required. In addition, Si nanowires have also been studied as potential materials for thermal diodes and transistors [10].

An accurate and detailed understanding of heat transport characteristics is critical for all the aforementioned applications, particularly in small dimensions where bulk-like approximations may be unreliable due to the prominent role of boundary scattering. Ultrathin nanowires, with diameters below 1 nm, are an intriguing model system in this regard, as they exhibit an extremely high surface-to-volume ratio, making boundary scattering the dominant factor ultimately controlling thermal transport properties. However, our understanding of thermal transport in these systems has been limited by the lack of experimental or reliable computational data for such small dimensions. As a matter of fact, the majority of experimental research has focused on larger Si nanowires with sizes ranging from 20 to 100 nm [11–13], while from a theoretical perspective, various studies, mainly based on classical molecular dynamics (MD), have been addressed to diameters greater than 1 nm [14–17] reporting conflicting results on the estimated thermal conductivity which has been found to critically depend on the adopted force field and/or the selected MD protocol.

Our study aims to fill this gap in the current literature by investigating the thermal transport properties of ultrathin Si [110] nanowires with a diameter $d \leq 1.5$ nm (although have not been synthesized yet). We focus in particular on the prediction of the $\kappa(d)$ trend based on state-of-the-art ab initio calculations. By this choice, we argue that two sources of limited accuracy are eliminated, namely the use of empirical force fields (each one with its questionable reliability) and the choice of MD protocol (each one with its drawback even if by means of MD anharmonicity at all orders are naturally accounted). Rather, we will solve the Boltzmann transport equation by using phonon-related information calculated at the density functional perturbation theory level [18].

Our calculations show a steady thermal conductivity reduction as the nanowire diameter decreases due to avoided-crossing phenomena [19–21] in the optical–acoustic phonon dispersion relations, mostly occurring for nanowires of small size. Furthermore, it is shown that even small changes in the diameter can have a considerable impact on the phonon dispersions, which in turn affect the scattering mechanisms. In addition, we provide evidence that a Casimir approximation of boundary scattering [22] leads to a

^a e-mail: claudio.melis@dsf.unica.it (corresponding author)

severe underestimation of thermal conductivity, proving that boundary scattering alone is insufficient to explain thermal transport effects for nanowires of such dimensions.

2 Theoretical framework

2.1 Simulated structures

The [110] direction has been chosen for the wire axis as it has been shown to be favored in various fabrication processes, in particular for small diameters [23–25]. To ensure the thermodynamic stability of the Si nanowires, we saturated the dangling bonds on the surface of the nanowires with hydrogen atoms, which prevents the formation of unwanted surface states [26]. It should be noted that while most prior studies have simulated Si nanowires in the [100] direction, we have focused on the more relevant [110] direction. Although similar trends are expected for nanowires in all high-symmetry directions, any quantitative comparison should be approached with caution. The size of the generated nanowires ranges from 0.38 to 1.5 nm corresponding to a total of 14 (6 Si, 8 H) to 62 (42 Si, 20 H) atoms in the unit cell, respectively. For each specific diameter, we perform both geometry and supercell volume minimization processes to obtain final structures with minimized stress and strain. Consequently, we end up with distinct lattice constants for each system under investigation. The lattice spacing in [110] direction resulted in $a = 5.476 \text{ \AA}$, 5.382 \AA , 5.404 \AA , 5.410 \AA , 5.380 \AA and 5.402 \AA for $d = 0.38 \text{ nm}$, 0.53 nm , 0.78 nm , 0.86 nm , 0.98 nm and 1.5 nm , respectively. This procedure ensures the overall stability of all the structures we examined. We remark that, while phonon dispersion curves have been calculated for any sample, the explicit calculation of the thermal conductivity was computationally feasible only for nanowires with a diameter up to 0.98 nm (54 atoms). The cross section of these nanowires is shown as insets in Fig. 3.

2.2 Computational details

All calculations have been carried out with the QUANTUM ESPRESSO program package [27, 28], which, including its plug-ins, provides all elements necessary for the calculation of the third-order interatomic force constants (IFC) and related phonon scattering rates providing the lattice thermal conductivity tensor $\kappa_L^{\alpha\beta}$ [29–31]

$$\kappa_L^{\alpha\beta} = \frac{\hbar^2}{N_0 \Omega k_B T^2} \sum_{\mathbf{q}j} c_{\mathbf{q}j}^{\alpha} c_{\mathbf{q}j}^{\beta} \omega_{\mathbf{q}j}^2 n_{\mathbf{q}j} (n_{\mathbf{q}j} + 1) \tau_{\mathbf{q}j} \quad (1)$$

where $c_{\mathbf{q}j}^{\alpha,\beta}$ are the branch-depending components of phonon group velocities along the α and β Cartesian directions, Ω is the unit cell volume, k_B is the Boltzmann constant and $\omega_{\mathbf{q}j}$, $n_{\mathbf{q}j}$ and $\tau_{\mathbf{q}j}$ are the vibrational frequencies, the occupation, and the relaxation time, respectively, of the corresponding phonon mode. Here, \mathbf{q} and j indicate the phonon wavevector and branch, and N_0 is the total number of \mathbf{q} points in the first Brillouin zone.

We remark an important issue relevant for the following discussion: the relaxation time $\tau_{\mathbf{q}j}$ is in principle obtained as the inverse of the sum of all scattering terms; in fact, in the present calculation only anharmonic scattering rates are considered since boundary scattering is naturally included in the explicit geometry of the simulated nanowires. A detailed description of the method has been provided previously [30, 32]. The volume Ω has been estimated by considering the average nanowire diameter excluding the external hydrogen atoms and vacuum region present in the unit cell. As evident from Fig. 3, the cross-sectional shape of the nanowires takes on an ellipsoidal form. Consequently, the determination of the nanowire diameter has been approximated as the mean value between the lengths of the two corresponding semiaxes.

The local density approximation and the PZ (Perdew–Zunger) [33] functional have been adopted to describe exchange and correlation terms, together with norm-conserving Troullier–Martins type pseudopotentials [34] for the description of interactions with the frozen cores. Monkhorst–Pack sampling has been used for the generation of the \mathbf{k} -point grid [35]. Electronic ground state calculations have been carried out using a $1 \times 1 \times 8$ \mathbf{k} -point grid (here \mathbf{k} is the electron wavevector). Phonon dispersion relations have been obtained using the PH module [36] of QUANTUM ESPRESSO with a $1 \times 1 \times 8$ \mathbf{q} -point grid in the [110] direction which has been verified to be sufficiently accurate for converged results. The self-consistent field convergence threshold for phonon calculations has been set to 10^{-18} Ry^2 . This threshold has been verified for the $d = 0.86 \text{ nm}$ nanowire to be sufficient for convergence of phonon modes.

Calculation of the scattering mechanisms and the thermal conductivity has been carried out using the THERMAL2 code of the D3Q plug-in [30] which provides third-order interatomic force constants from density functional perturbation theory (DFPT) [37–41]. For the determination of scattering terms, a $1 \times 1 \times 120$ \mathbf{q} -point grid has been applied and the smearing parameter for energy conservation has been set to 1 cm^{-1} . The grid density and smearing parameter have been adjusted on the example of the $d = 0.73 \text{ nm}$ nanowire. This computational setup resulted in a huge computational burden as shown in Table 1.

Table 1 Wall-time (hours) estimates for each DFPT calculation

d (nm)	Atoms	Cores	Wall-time (hours)
0.38	14	192	1:21
0.73	16	192	2:32
0.78	27	192	11:25
0.86	28	192	12:49
0.98	54	192	59:31
1.5	62	192	167:09

3 Results

3.1 Phonon dispersion relations and scattering mechanisms

In the one-dimensional nanowire structure, there are four acoustic modes, namely, one rotational mode, one longitudinal mode and two bending modes [42]. The rotational mode, which corresponds to a torsion of the nanowire, and the longitudinal mode, which corresponds to a displacement along the wire axis, have a linear dispersion for $\mathbf{q} \rightarrow 0$. The other two modes, corresponding to displacements orthogonal to the wire axis (flexural modes), are instead quadratic as extensively discussed in [43].

Figure 1 shows the phonon dispersion relations of a Si [110] nanowire with a diameter of 0.86 nm in comparison with the dispersion relations in bulk Si in the corresponding direction. For a better visualization, we show phonon frequencies only up to 8 THz, keeping in mind that low-frequency phonons are dominant in thermal transport in such systems. Vibrational frequencies of acoustic modes in the nanowire are lower with respect to bulk Si and result to be in good agreement to previous computational studies, so proving evidence of the reliability of the present computational setup [16, 42].

If diameters are above 1–2 nm, an increase in the thermal conductivity with respect to a thickness increase is generally observed. While this behavior (where the smaller is the diameter, the smaller is the thermal conductivity) is at odd with what reported for other Si-based nanosystems [44–48], it has been confirmed in GaP nanowires [49]. This intriguing feature has been attributed to an increase in frequency of the lowest optical modes at the zone center with decrease in wire diameter which reduces the available channels for Umklapp scattering at low frequencies [16, 49]. A similar behavior has been verified in the systems here investigated as shown in Fig. 2 for $0.38 \leq d \leq 1.5$ nm, while the zone center optical frequency is found to decrease from 2.2 to 1.4 THz, respectively.

Explicit calculation of the phonon dispersion scattering terms using DFPT is a very demanding computational task. Therefore, the number of the investigated nanowires has been reduced, corresponding to five systems with $0.38 \text{ nm} \leq d \leq 0.95$ nm. It was expected to find less scattering channels with decrease in nanowire diameter as a result of the higher optical bands (leading to a decrease in Umklapp scattering as described above [16, 49]). On the contrary, just the opposite trend has been found. As shown in Fig. 2, we in fact observe that by decreasing the nanowire diameter the lower optical bands mix with the acoustic branches. The phenomenon, named “avoided-crossing” [19–21], affects the acoustic and low-lying optical phonons by strongly increasing vibrational anharmonicity, a feature which eventually reduces κ_L . Furthermore, any avoided-crossing flattens the phonon bands, lowering the group velocity of acoustic phonons and thus further reducing the lattice thermal conductivity. This is clearly shown in Fig. 2. Such a band flattening is more evident in thinner nanowires.

For most of the investigated samples, we observe a corresponding increase in the phonon scattering rate (Fig. 3). The significant reduction in phonon lifetime observed in the nanowire with the smallest diameter can be explained in terms of surface-to-volume effects. As the nanowire diameter decreases, the proportion of atoms located at the surface increases. Additionally, it is widely recognized that surface vibrations exhibit a stronger anharmonicity due to the broken symmetry at the surface, leading to phonon scattering rates higher than those found in the bulk [50]. Consequently, in the case of the smallest d values, nearly all the atoms are situated at the surface, resulting in all vibrational modes being highly anharmonic.

Finally, Fig. 4 shows the average phonon mean free path (mfp) as a function of the nanowire’s diameter. We observe significant mfp reduction for all the nanowires compared to bulk silicon, where it typically reaches a few microns [51]. Additionally, we observe that mfp is considerably larger than the diameter. This finding provides compelling evidence that the sole Casimir effect falls short in explaining thermal conductivities in Si nanowires. Specifically, the Casimir effect assumes that all phonons with mean free paths greater than the nanowire diameter would be effectively scattered out of the system. However, our work reveals a more intricate scenario: varying the nanowires diameter has the potential to profoundly alter both the harmonic phonon branches and the anharmonic phonon properties. Such features have a substantial impact on the resulting thermal conductivity characteristics of the nanowire.

Fig. 1 Phonon dispersion relations of Si [110] nanowires (red lines) with $d = 0.86$ nm and in bulk Si (blue lines) in the corresponding direction

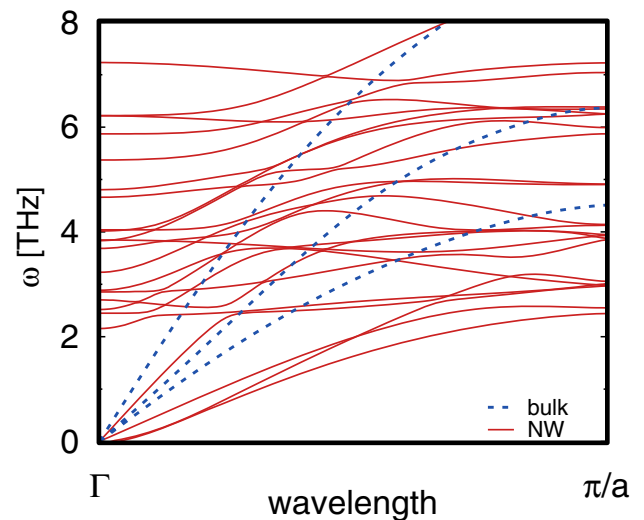
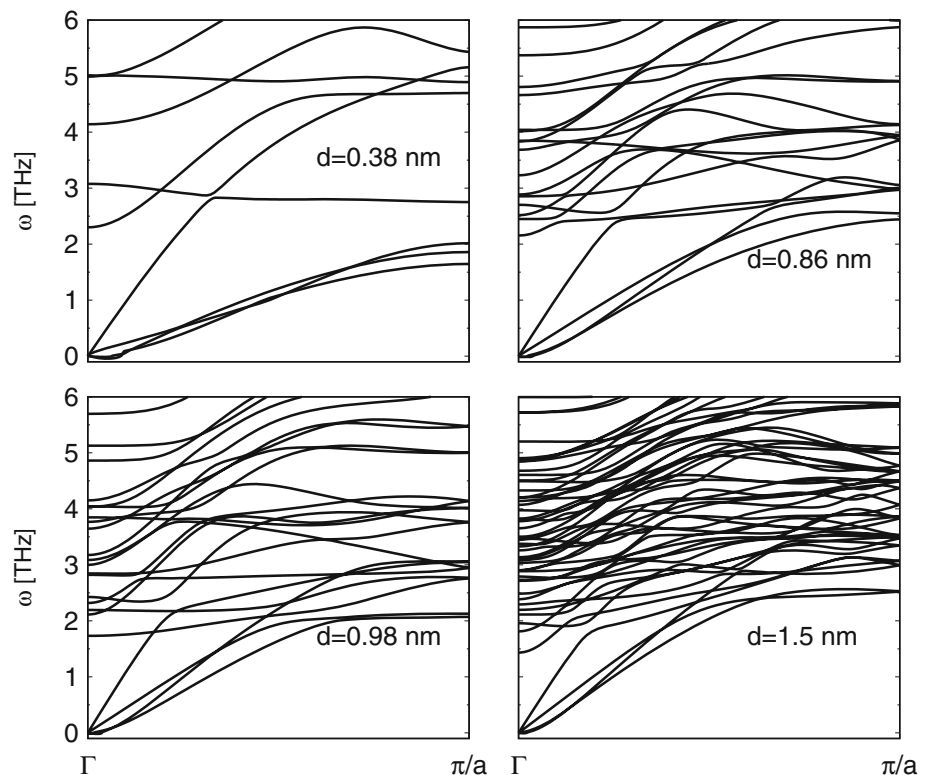


Fig. 2 Phonon dispersion of Si nanowires in [110] direction with average diameter of 0.38, 0.86, 0.98 and 1.5 nm

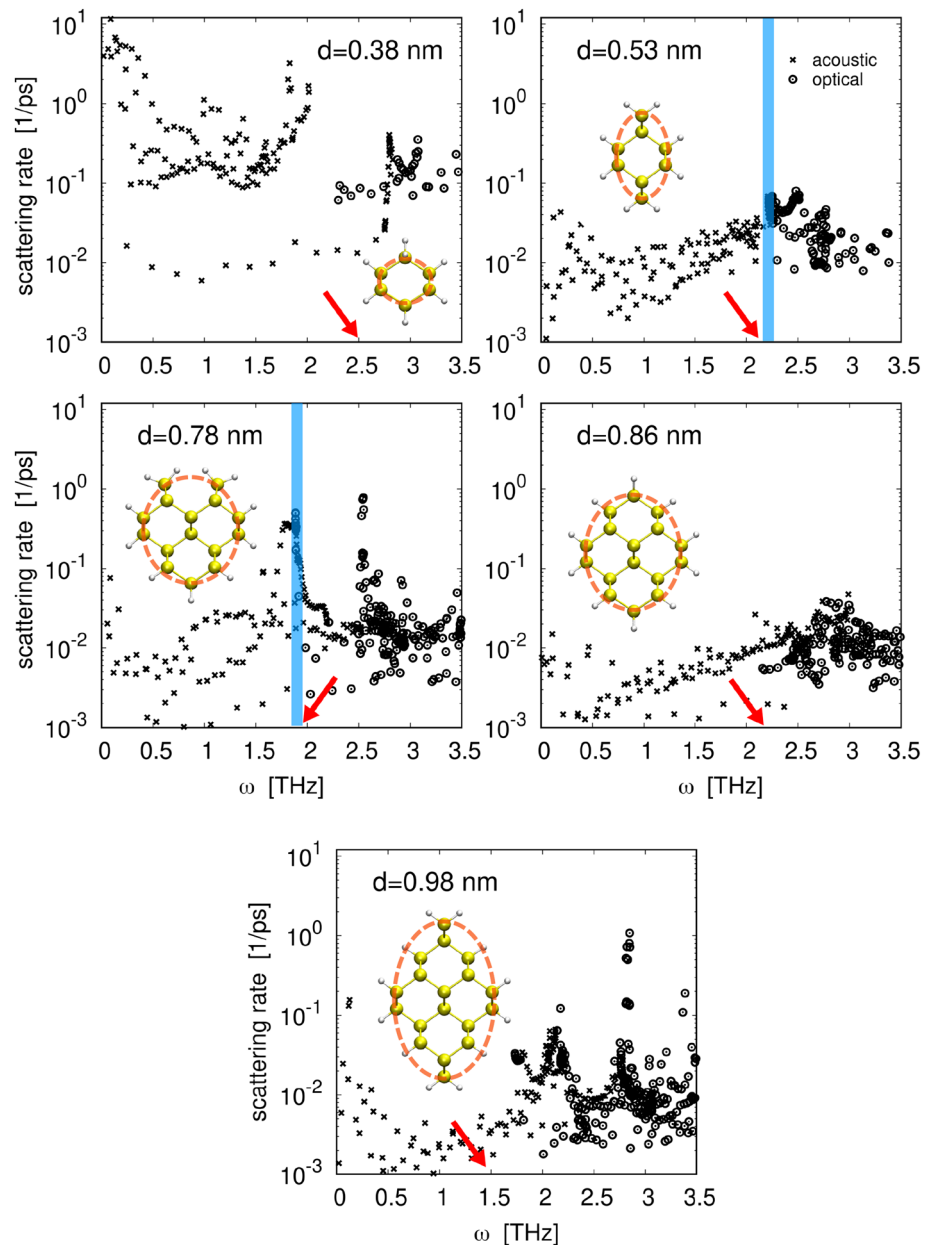


3.2 Thermal conductivity

Based on the phonon dispersions and the scattering rates described above, the thermal conductivity at $T = 300$ K has been calculated for $0.38 \text{ nm} \leq d \leq 0.98 \text{ nm}$. For these diameters, the thermal conductivity is found to increase almost linearly from 40 to $119 \text{ Wm}^{-1} \text{ K}^{-1}$ as shown in Fig. 5.

This is in contrast to previous studies that showed an increase of κ_L by decreasing d [16, 49] $d = 2$ nm. However, it should be noted that diameters of the nanowires calculated here are below the smallest size of the previous studies. In fact, the thermal conductivity of the 0.98 nm sample is in reasonable agreement with Donadio et al. [15]. As discussed above, additional and increased scattering is found in the thinnest nanowires here investigated which eventually dominate over Normal scattering events. We argue that a maximum of thermal conductivity is likely present around 1 nm. In thinner nanowires, boundary scattering and the band flattening (resulting from avoided-crossing) become dominant, leading to a linear reduction of thermal conductivity with decrease in diameter. Besides the different diameters investigated, we believe that the discrepancies observed in thermal conductivities can

Fig. 3 Phonon scattering rates of acoustic (crosses) and optical (circles) modes in Si [110] nanowires with an average diameter of 0.38 nm, 0.53 nm, 0.78 nm, 0.86 nm and 0.98 nm. Red arrows indicate optical phonons with the lowest energy at Γ and the vertical blue lines highlight the frequency where notable alignment of phonon modes is present (see Fig. 2). Insets show the cross section of the corresponding sample where the red dotted line has been added in order to mark the selected cross-sectional shape of the nanowires



be attributed to the fact that references [16, 49] employ empirical potentials to sample the interatomic interactions, as opposed to this work where ab initio DFT calculations have been employed.

In order to estimate the effect of boundary scattering, we also calculated κ_L using the Casimir approximation [22] (Fig. 5): while anharmonic phonon scattering is obtained from the bulk phonon structure, size effects are phenomenologically described as additional boundary scattering terms. As shown in Fig. 5, the Casimir method notably underestimates the thermal conductivity with respect its explicit calculation. This confirms that only considering boundary scattering is not able to correctly describe all effects ruling over thermal transport in ultrathin nanowires. Instead, an accurate representation of the phonon dispersion is necessary in order to quantitatively account all features affecting phonon interactions.

4 Conclusions

In summary, ultrathin Si nanowires and their phonon characteristics have been investigated using density functional perturbation theory. The phonon dispersion is discussed for nanowires in [110] direction with a diameter ranging from 0.38 to 1.5 nm.

Fig. 4 Average phonon mean free path (mfp) of Si nanowires in [110] direction as a function of the corresponding average diameter

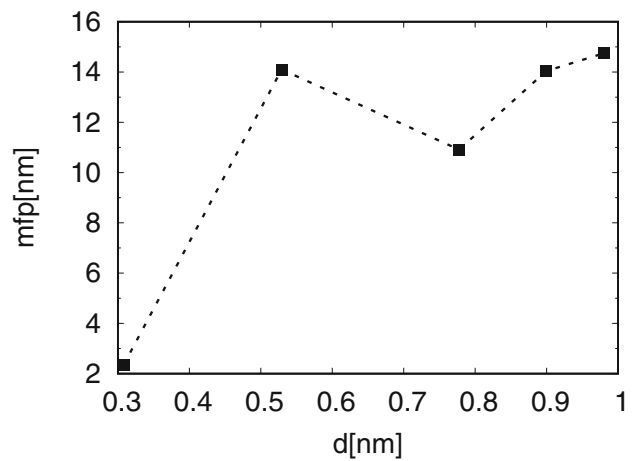
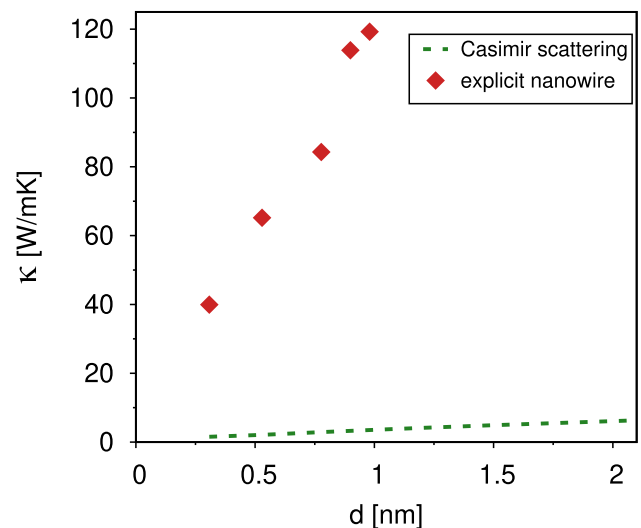


Fig. 5 Thermal conductivity in ultrathin Si nanowires in [110] direction calculated explicitly (red diamonds) in comparison with results using the Casimir model (green broken line) where only boundary scattering is considered



A general trend has been found that the thermal conductivity decreases from $119 \text{ Wm}^{-1} \text{ K}^{-1}$ down to $40 \text{ Wm}^{-1} \text{ K}^{-1}$ by reducing the nanowire diameter from 0.98 nm to 0.38 nm. In addition, it is shown that small changes in the diameter of ultrathin nanowires can lead to drastic changes in the phonon dispersions which eventually deeply affect the scattering mechanisms. In fact, by modeling boundary scattering through phenomenological Casimir method (still using bulk-like phonon dispersions) notably underestimates the results obtained by explicit calculations. This provides evidence that boundary scattering alone cannot explain thermal transport effects in those ultrathin systems here investigated. Rather, we have shown that it is crucial to rely on an explicit and correct description of the phonon dispersions: as a matter of fact, their complex topology plays indeed a major role.

Acknowledgements One of us (KH) acknowledges financial support by Ministero dell'Università e Ricerca (MIUR) under the Piano Operativo Nazionale 2014–2020 asse I, action I.2 “Mobilità dei Ricercatori” (PON 2014–2020, AIM), through project AIM1809115-1. One of us (LC) acknowledges financial support under the National Recovery and Resilience Plan (NRRP), Mission 4 Component 2 Investment 1.3—Call for tender No.341 published on March 13, 2022, by the Italian Ministry of University and Research (MUR) funded by the European Union—NextGenerationEU. Award Number: Project code PE 00000021, Con- cession Decree No. 1561 adopted on October 11, 2022 by the Italian Ministry of Ministry of University and Research (MUR), CUP F53C22000770007, Project title “NEST—Network 4 Energy Sustainable Transition.”

Funding Open access funding provided by Università degli Studi di Cagliari within the CRUI-CARE Agreement.

Data Availability Statement This manuscript has associated data in a data repository. [Authors' comment: The datasets generated during and/or analysed during the current study are available from the corresponding author on reasonable request].

Open Access This article is licensed under a Creative Commons Attribution 4.0 International License, which permits use, sharing, adaptation, distribution and reproduction in any medium or format, as long as you give appropriate credit to the original author(s) and the source, provide a link to the Creative Commons licence, and indicate if changes were made. The images or other third party material in this article are included in the article's Creative Commons licence, unless indicated otherwise in a credit line to the material. If material is not included in the article's Creative Commons licence and your intended use is not permitted by statutory regulation or exceeds the permitted use, you will need to obtain permission directly from the copyright holder. To view a copy of this licence, visit <http://creativecommons.org/licenses/by/4.0/>.

References

1. R. Rurali, Colloquium: structural, electronic, and transport properties of silicon nanowires. *Rev. Mod. Phys.* **82**(1), 427–449 (2010). <https://doi.org/10.1103/REVMODPHYS.82.427/FIGURES/12/MEDIUM>
2. R. Chen, J. Lee, W. Lee, D. Li, Thermoelectrics of nanowires. *Chem. Rev.* **119**(15), 9260–9302 (2019)
3. S.K. Ray, A.K. Katiyar, A.K. Raychaudhuri, One-dimensional Si/Ge nanowires and their heterostructures for multifunctional applications—a review. *Nanotechnology* **28**(9), 092001 (2017)
4. K.Q. Peng, X. Wang, L. Li, Y. Hu, S.T. Lee, Silicon nanowires for advanced energy conversion and storage. *Nano Today* **8**(1), 75–97 (2013). <https://doi.org/10.1016/J.NANTOD.2012.12.009>
5. T. Mikolajick, A. Heinzig, J. Trommer, S. Pregl, M. Grube, G. Cuniberti, W.M. Weber, Silicon nanowires—a versatile technology platform. *Phys. Status Solidi Rapid Res. Lett.* **7**(10), 793–799 (2013). <https://doi.org/10.1002/PSSR.201307247>
6. G. Zhang, Y.W. Zhang, Thermal conductivity of silicon nanowires: from fundamentals to phononic engineering. *Phys. Status Solidi Rapid Res. Lett.* **7**(10), 754–766 (2013). <https://doi.org/10.1002/PSSR.201307188>
7. M.C. Browne, B. Norton, S.J. McCormack, Phase change materials for photovoltaic thermal management. *Renew. Sustain. Energy Rev.* **47**, 762–782 (2015). <https://doi.org/10.1016/J.RSER.2015.03.050>
8. M.Y. Wong, C.Y. Tso, T.C. Ho, H.H. Lee, A review of state of the art thermal diodes and their potential applications. *Int. J. Heat Mass Transf.* **164**, 120607 (2021). <https://doi.org/10.1016/J.IJHEATMASSTRANSFER.2020.120607>
9. D.G. Cahill, W.K. Ford, K.E. Goodson, G.D. Mahan, A. Majumdar, H.J. Maris, R. Merlin, S.R. Phillpot, Nanoscale thermal transport. *J. Appl. Phys.* **93**(2), 793–818 (2003). <https://doi.org/10.1063/1.1524305>
10. X. Cartoixa, L. Colombo, R. Rurali, Thermal rectification by design in telescopic Si nanowires. *Nano Lett.* **15**(12), 8255–8259 (2015). <https://doi.org/10.1021/ACS.NANO.5B03781>
11. D. Li, Y. Wu, P. Kim, L. Shi, P. Yang, A. Majumdar, Thermal conductivity of individual silicon nanowires. *Appl. Phys. Lett.* **83**(14), 2934 (2003). <https://doi.org/10.1063/1.1616981>
12. A.I. Hochbaum, R. Chen, R.D. Delgado, W. Liang, E.C. Garnett, M. Najarian, A. Majumdar, P. Yang, Enhanced thermoelectric performance of rough silicon nanowires. *Nature* **451**(7175), 163–167 (2008). <https://doi.org/10.1038/nature06381>
13. V. Poborchii, Y. Morita, J. Hattori, T. Tada, P.I. Geshev, Corrugated Si nanowires with reduced thermal conductivity for wide-temperature-range thermoelectricity. *J. Appl. Phys.* **120**(15), 154304 (2016). <https://doi.org/10.1063/1.4965302>
14. S.G. Volz, G. Chen, Molecular dynamics simulation of thermal conductivity of silicon nanowires. *Appl. Phys. Lett.* **75**(14), 2056 (1999). <https://doi.org/10.1063/1.124914>
15. D. Donadio, G. Galli, Temperature dependence of the thermal conductivity of thin silicon nanowires. *Nano Lett.* **10**(3), 847–851 (2010). https://doi.org/10.1021/NL903268Y/ASSET/IMAGES/MEDIUM/NL-2009-03268Y_0004.GIF
16. Y. Zhou, X. Zhang, M. Hu, Nonmonotonic diameter dependence of thermal conductivity of extremely thin Si nanowires: competition between hydrodynamic phonon flow and boundary scattering. *Nano Lett.* **17**(2), 1269–1276 (2017). https://doi.org/10.1021/ACS.NANO.6B05113/SUPPL_FILE/NL6B05113_SI_001.PDF
17. Z. Wang, N. Mingo, Diameter dependence of SiGe nanowire thermal conductivity. *Appl. Phys. Lett.* **97**(10), 101903 (2010). <https://doi.org/10.1063/1.3486171>
18. G. Fugallo, L. Colombo, Calculating lattice thermal conductivity: a synopsis. *Phys. Scr.* **93**(4), 043002 (2018)
19. M. Christensen, A.B. Abrahamsen, N.B. Christensen, F. Juranyi, N.H. Andersen, K. Lefmann, J. Andreasson, C.R.H. Bahl, B.B. Iversen, Avoided crossing of rattler modes in thermoelectric materials. *Nat. Mater.* **7**(10), 811–815 (2008). <https://doi.org/10.1038/nmat2273>
20. W. Li, J. Carrete, G.K.H. Madsen, N. Mingo, Influence of the optical-acoustic phonon hybridization on phonon scattering and thermal conductivity. *Phys. Rev. B* **93**(20), 205203 (2016). <https://doi.org/10.1103/PHYSREVB.93.205203/FIGURES/4/MEDIUM>
21. Y. Li, S. Yamamoto, K. Ahmad, Z. Almutairi, K. Koumoto, C. Wan, Localized vibration and avoided crossing in SrTi11020 for oxide thermoelectrics with intrinsically low thermal conductivity. *J. Mater. Chem. A* **9**(19), 11674–11682 (2021). <https://doi.org/10.1039/D1TA01920A>
22. H.B.G. Casimir, Note on the conduction of heat in crystals. *Physica* **5**(6), 495–500 (1938). [https://doi.org/10.1016/S0031-8914\(38\)80162-2](https://doi.org/10.1016/S0031-8914(38)80162-2)
23. C.-P. Li, C.-S. Lee, X.-L. Ma, N. Wang, R.-Q. Zhang, S.-T. Lee, Growth direction and cross-sectional study of silicon nanowires. *Adv. Mater.* **15**(7–8), 607–609 (2003). <https://doi.org/10.1002/ADMA.200304409>
24. Y. Wu, Y. Cui, L. Huynh, C.J. Barrelet, D.C. Bell, C.M. Lieber, Controlled growth and structures of molecular-scale silicon nanowires. *Nano Lett.* **4**(3), 433–436 (2004). <https://doi.org/10.1021/nl035162i>
25. R.Q. Zhang, Y. Lifshitz, D.D.D. Ma, Y.L. Zhao, T. Frauenheim, S.T. Lee, S.Y. Tong, Structures and energetics of hydrogen-terminated silicon nanowire surfaces. *J. Chem. Phys.* **123**(14), 144703 (2005). <https://doi.org/10.1063/1.2047555>
26. R. Zhang, Y. Lifshitz, D. Ma, Y. Zhao, T. Frauenheim, S. Lee, S. Tong, Structures and energetics of hydrogen-terminated silicon nanowire surfaces. *J. Chem. Phys.* **123**(14), 144703 (2005)
27. P. Giannozzi, S. Baroni, N. Bonini, M. Calandra, R. Car, C. Cavazzoni, D. Ceresoli, G.L. Chiarotti, M. Cococcioni, I. Dabo, A. Dal Corso, S. de Gironcoli, S. Fabris, G. Fratesi, R. Gebauer, U. Gerstmann, C. Gougoussis, A. Kokalj, M. Lazzeri, L. Martin-Samos, N. Marzari, F. Mauri, R. Mazzarello, S. Paolini, A. Pasquarello, L. Paulatto, C. Sbraccia, S. Scandolo, G. Sclauzero, A.P. Seitsonen, A. Smogunov, P. Umari, R.M. Wentzcovitch, QUANTUM ESPRESSO: a modular and open-source software project for quantum simulations of materials. *J. Phys. Condens. Matter* **21**(39), 395502 (2009). <https://doi.org/10.1088/0953-8984/21/39/395502>
28. P. Giannozzi, O. Andreussi, T. Brumme, O. Bunau, M. Buongiorno Nardelli, M. Calandra, R. Car, C. Cavazzoni, D. Ceresoli, M. Cococcioni, N. Colonna, I. Carnimeo, A. Dal Corso, S. de Gironcoli, P. Delugas, R.A. Distasio, A. Ferretti, A. Floris, G. Fratesi, G. Fugallo, R. Gebauer, U. Gerstmann, F. Giustino, T. Gorni, J. Jia, M. Kawamura, H.Y. Ko, A. Kokalj, E. Küçükbenli, M. Lazzeri, M. Marsili, N. Marzari, F. Mauri, N.L. Nguyen, H.V. Nguyen, A. Otero-De-La-Roza, L. Paulatto, S. Poncé, D. Rocca, R. Sabatini, B. Santra, M. Schlipf, A.P. Seitsonen, A. Smogunov, I. Timrov, T. Thonhauser, P. Umari, N. Vast, X. Wu, S. Baroni, Advanced capabilities for materials modelling with Quantum ESPRESSO. *J. Phys. Condens. Matter* **29**(46), 465901 (2017). <https://doi.org/10.1088/1361-648X/AA8F79>
29. G. Fugallo, M. Lazzeri, L. Paulatto, F. Mauri, Ab initio variational approach for evaluating lattice thermal conductivity. *Phys. Rev. B Condens. Matter Mater. Phys.* **88**(4), 045430 (2013). <https://doi.org/10.1103/PhysRevB.88.045430>
30. L. Paulatto, F. Mauri, M. Lazzeri, Anharmonic properties from a generalized third-order ab initio approach: theory and applications to graphite and graphene. *Phys. Rev. B* **87**(21), 214303 (2013). <https://doi.org/10.1103/PhysRevB.87.214303>
31. J.M. Ziman, *Electrons and Phonons: The Theory of Transport Phenomena in Solids* (Clarendon, Oxford, 1960)
32. K.R. Hahn, C. Melis, F. Bernardini, L. Colombo, Engineering the thermal conductivity of doped SiGe by mass variance: a first-principles proof of concept. *Front. Mech. Eng.* **7**, 66 (2021). <https://doi.org/10.3389/FMECH.2021.712989/BIBTEX>

33. J.P. Perdew, A. Zunger, Self-interaction correction to density-functional approximations for many-electron systems. *Phys. Rev. B* **23**(10), 5048 (1981). <https://doi.org/10.1103/PhysRevB.23.5048>
34. N. Troullier, J.L. Martins, Efficient pseudopotentials for plane-wave calculations. *Phys. Rev. B* **43**(3), 1993–2006 (1991). <https://doi.org/10.1103/PhysRevB.43.1993>
35. H.J. Monkhorst, J.D. Pack, Special Points for Brillouin-Zone Integrations. *Phys. Rev. B* **13**(12), 5188–5192 (1976)
36. A. Dal Corso, S. Baroni, R. Resta, S. de Gironcoli, Ab initio calculation of phonon dispersions in II–VI semiconductors. *Phys. Rev. B* **47**(7), 3588 (1993). <https://doi.org/10.1103/PhysRevB.47.3588>
37. S. Baroni, P. Giannozzi, A. Testa, Green's-function approach to linear response in solids. *Phys. Rev. Lett.* **58**(18), 1861–1864 (1987). <https://doi.org/10.1103/PhysRevLett.58.1861>
38. P. Giannozzi, S. de Gironcoli, P. Pavone, S. Baroni, Ab initio calculation of phonon dispersions in semiconductors. *Phys. Rev. B* **43**(9), 7231–7242 (1991). <https://doi.org/10.1103/PhysRevB.43.7231>
39. S. Baroni, S. de Gironcoli, A. Dal Corso, P. Giannozzi, Phonons and related crystal properties from density-functional perturbation theory. *Rev. Mod. Phys.* **73**(2), 515–562 (2001). <https://doi.org/10.1103/RevModPhys.73.515>
40. A. Debernardi, S. Baroni, Third-order density-functional perturbation theory: a practical implementation with applications to anharmonic couplings in Si. *Solid State Commun.* **91**(10), 813–816 (1994). [https://doi.org/10.1016/0038-1098\(94\)90654-8](https://doi.org/10.1016/0038-1098(94)90654-8)
41. A. Debernardi, S. Baroni, E. Molinari, Anharmonic phonon lifetimes in semiconductors from density-functional perturbation theory. *Phys. Rev. Lett.* **75**(9), 1819–1822 (1995). <https://doi.org/10.1103/PhysRevLett.75.1819>
42. H. Peelaers, B. Partoens, F.M. Peeters, Phonon band structure of Si nanowires: a stability analysis. *Nano Lett.* **9**(1), 107–111 (2009). <https://doi.org/10.1021/nl802613p>
43. Y. Kuang, L. Lindsay, Q. Wang, L. He, Lattice chain theories for dynamics of acoustic flexural phonons in nonpolar nanomaterials. *Phys. Rev. B* **102**(14), 144301 (2020)
44. C. Melis, L. Colombo, Lattice thermal conductivity of $\text{Si}_{1-x}\text{Ge}_x$ nanocomposites. *Phys. Rev. Lett.* **112**(6), 065901 (2014). <https://doi.org/10.1103/PhysRevLett.112.065901>
45. S.K. Bux, R.G. Blair, P.K. Gogna, H. Lee, G. Chen, M.S. Dresselhaus, R.B. Kaner, J.P. Fleurial, Nanostructured bulk silicon as an effective thermoelectric material. *Adv. Funct. Mater.* **19**(15), 2445–2452 (2009). <https://doi.org/10.1002/adfm.200900250>
46. H. Lee, D. Vashaee, D.Z. Wang, M.S. Dresselhaus, Z.F. Ren, G. Chen, Effects of nanoscale porosity on thermoelectric properties of SiGe. *J. Appl. Phys.* **107**(9), 094308 (2010). <https://doi.org/10.1063/1.3388076>
47. I. Savic, D. Donadio, F. Gygi, G. Galli, Dimensionality and heat transport in Si–Ge superlattices. *Appl. Phys. Lett.* **102**(7), 073113 (2013). <https://doi.org/10.1063/1.4792748>
48. R. Cheaito, J.C. Duda, T.E. Beechem, K. Hattar, J.F. Ihlefeld, D.L. Medlin, M.A. Rodriguez, M.J. Campion, E.S. Piekos, P.E. Hopkins, Experimental investigation of size effects on the thermal conductivity of silicon–germanium alloy thin films. *Phys. Rev. Lett.* **109**(19), 195901 (2012). <https://doi.org/10.1103/PhysRevLett.109.195901>
49. S. Gireesan, P. Torres, F.X. Alvarez, P.A. Bobbert, Diameter-dependent thermal conductivity of ultrathin GaP nanowires: a molecular dynamics study. *Phys. Rev. B* **101**(2), 024307 (2020). <https://doi.org/10.1103/PhysRevB.101.024307>
50. A. Baddorf, E. Plummer, Enhanced surface anharmonicity observed in vibrations on Cu (110). *Phys. Rev. Lett.* **66**(21), 2770 (1991)
51. R. Gereth, K. Hubner, Phonon mean free path in silicon between 77 and 250°k. *Phys. Rev.* **134**, 235–240 (1964). <https://doi.org/10.1103/PhysRev.134.A235>